Structural and magnetic properties of stoichiometric Co_4N epitaxial thin films

Nidhi Pandey,[1] Mukul Gupta,[1,*] Rachana Gupta,[2] Zaineb Hussain,[1] V. R. Reddy,[1] D. M. Phase,[1] and Jochen Stahn[3]

[1]*UGC-DAE Consortium for Scientific Research, University Campus, Khandwa Road, Indore 452 001, India*

[2]*Institute of Engineering and Technology DAVV, Khandwa Road, Indore 452 017, India*

[3]*Laboratory for Neutron Scattering and Imaging, Paul Scherrer Institut, CH-5232 Villigen PSI, Switzerland*

(Received 3 August 2018; published 26 June 2019)

In this work, we measured N self-diffusion in the Co-N system and found an unexpected result that N diffuses out almost completely around 500 K, leaving behind fcc Co irrespective of the amount of N used to deposit Co-N. On the other hand, in previous attempts the Co_4N phase has always been grown at 550 K or above. In view of our finding, it appears that fcc Co could have been mistaken for Co_4N, probably due to the closeness of their lattice parameters (LP; fcc Co = 3.54 Å, Co_4N= 3.74 Å). Therefore, Co_4N – an interesting material for its high spin-polarization ratio and high magnetic moment remained unexplored. By bringing down the growth temperature, we report the growth of stoichiometric Co_4N epitaxial thin films. Films were grown using a direct current reactive magnetron sputtering process on $LaAlO_3$ (LAO mismatch 1.4%) and MgO (mismatch 11.3%) substrates and their structural and magnetic properties were studied. Precise magnetic moment (M_s) of Co_4N samples were measured using polarized neutron reflectivity and compared with bulk magnetization results. We found that the M_s of Co_4N is higher due to a magnetovolume effect. Unlike previous findings, we observed that substrates induce misfit strain and strain inhomogeneity is the cause of modifications in magnetic ensemble such as coercivity, saturation magnetization, and magnetic anisotropy. A consequence of incoherent strain present in our samples is also reflected in the magnetic anisotropy leading to a superposition of strong fourfold and a small fraction of uniaxial magnetic anisotropy. Obtained results are presented and discussed in this work.

DOI: 10.1103/PhysRevB.99.214109

I. INTRODUCTION

Spintronics and high density magnetic memory devices demand a class of materials which primarily exhibit high spin polarization ratio (SPR), high saturation magnetism (M_s), low coercivity (H_c) etc. at room temperature [1]. In view of this, prominent ferromagnetic materials such as binary or ternary alloys of transition metals and rare earth intermetallic compounds, Heusler alloys, Mn and Cr based alloys [2–8] etc. have been actively pursued by several researchers. In addition, nitrides of 3*d* magnetic transition metals, binary and ternary rare-earth intermetallic compounds were also substantially investigated and recognized as efficient candidates for magnetic devices [5,9].

In particular, tetra metals nitrides (M_4N; M = Fe, Co, Ni, Mn) are a relatively new class of compounds that exhibit superior spintronic properties. They all share a similar type antiperovskite structure (space group; $Pm\bar{3}m$) in which the N atom occupies the central position as shown in Fig. 1. Such insertion of N increases the lattice volume leading to an enhancement in *Ms* [9,10] and a strong hybridization between N and M atoms results in high SPR [11]. Among M_4N, Fe_4N is well studied and predicted to have $M_s \approx 2.5\,\mu_B$/Fe atom [12], SPR ≈60% [11,13] and a gigantic value of tunnel magnetoresistance (TMR) ratio ≈24 000% [14]. Most of these have been verified experimentally in epitaxially grown Fe_4N thin films [15–17].

Recent theoretical reports on Co_4N predict even promising magnetic properties with SPR increasing to as high as ≈90% [13] with M_s (≈1.6 μ_B/Co atom) [18] and TMR (≈1260%) [14]. With low H_c and corrosion resistance, Co_4N is poised to be a superior candidate in spintronic devices. Recently, in a theoretical study Meinert *et al.* studied exchange interactions and did Monte Carlo simulations to calculated the Curie temperature (T_c) and found it to be 291 K (Cr_4N), 710 K (Mn_4N), 668 K (Fe_4N), 827 K (Co_4N), and 121 K (Ni_4N) [10]. As can be seen here among these compounds the T_c is highest in Co_4N at 827 K. Such multiple magnetic functionalities of Co_4N can harness the research in development of new families of spintronic devices and arise as rivals among promising ferromagnetic materials. However, as even the phase diagram of the Co-N has not been established yet, the recipe for formation of Co_4N phase is ambiguous. Due to this, the Co_4N has not been explored much experimentally and the available experimental reports are contradicting, e.g., the lattice parameter (LP) of Co_4N have been found between 3.59 to 3.52 Å [19–27] while its theoretical value is 3.735 Å [18]. Similarly, the M_s of Co_4N was found to vary in a rather large range between 485 and 1300emu/cm^3 [20,21,23–28]. Since the LP of fcc Co is about 3.54 Å [18], it appears that Co_4N thin films prepared so far might have a significant fraction of fcc Co. Theoretically, it is expected that N *at*.% tend to decreases monotonically with LP [18,29] and therefore, a correlation can be made between the substrate temperature (T_s) used to deposit Co_4N and their corresponding measured LP. We find that T_s between 435 to 725 K have been used and it apparently looks that as T_s is raised N diffuses out from

*Corresponding author: mgupta@csr.res.in

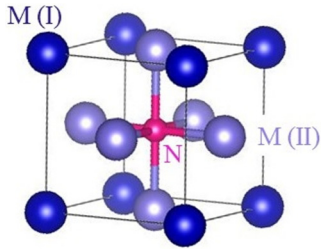

FIG. 1. Structure of M_4N compound with M = Fe, Co, Ni, Mn. The two inequivalent metal sites M(I) and M(II) adopt an antiperovskite structure as $M(I)M(II)_3N$.

the system, leaving behind fcc Co. But this is not unexpected, considering high (theoretical) enthalpy of formation, $\Delta H_f^\circ = 0 \pm 2.9$ kJ/mol for Co_4N [30,31]. Though the T_c of Co_4N is quite high at 827 K, its poor thermal stability is a concern. It can be anticipated that by using suitable dopants, the thermal stability of Co_4N can be improved following a similar approach achieved in Fe-X-N [32].

In this work, we studied the N self-diffusion process and used it to grow stoichiometric Co_4N epitaxial thin films. We found that the substrate induced misfit strain is an important factor in affecting the structural and magnetic properties of Co_4N films. The effect of strain inhomogeneity on magnetic properties especially in terms of their magnetic anisotropy are presented and discussed.

II. EXPERIMENT

Co_4N thin films (≈120 nm) were prepared on $LaAlO_3$ and MgO substrates using a direct current magnetron sputtering system (Orion-8, AJA Int. Inc.) at ambient temperature (≈300 K). A Co target (99.95%) (ϕ = 1 inch) was sputtered. The partial pressure of nitrogen gas flow (R_{N_2}) was fixed at 12%; here $R_{N_2} = p_{N_2}/(p_{Ar} + p_{N_2})$; p_{Ar} and p_{N_2} are gas flow of Ar and N_2 gases, respectively. A base pressure of 1×10^{-7} Torr was achieved before deposition and the working pressure was maintained at 3 mTorr during deposition. More details about sample preparation can be found elsewhere [33–35].

Deposited samples were characterized for their long range ordering and phase formation by x-ray diffraction (XRD) using a standard x-ray diffractometer (Bruker D8 Advance) having Cu-Kα x-ray source. Reciprocal space mapping (RSM) and Phi scans were performed with high resolution x-ray diffractometer (Bruker D8 Discover). N self-diffusion was measured on a separate sample in which a $Co^{15}N$ layer was sandwiched between thick CoN layers. ^{15}N depth profiles were measured using secondary ion mass spectroscopy (SIMS) in a Hiden Analytical SIMS workstation. A primary O_2^+ ions source was used for sputtering with an energy of 5 keV and beam current of 400 nA. The sputtered secondary ions were detected using a quadrupole mass analyzer. Polarized neutron reflectivity (PNR) measurements were performed at AMOR, SINQ, PSI Switzerland in time of flight mode using Selene optics [36,37], which allows us to focus a beam of neutrons so that PNR measurements can be done on smaller samples ($\leqslant 1$ cm^2). During PNR measurements, to saturate the sample magnetically, a magnetic field of 0.5 T was applied parallel to the sample surface. Magnetic anisotropy was studied using magneto-optical Kerr effect (MOKE) and Kerr microscopy (Evico Magnetics) equipment.

III. RESULTS AND DISCUSSION

In order to understand the formation of cobalt nitride (Co-N) phases, the knowledge of N self-diffusion process is essential but it has not yet been studied. Self-diffusion process is defined as the atomic diffusion in the absence of any chemical potential gradient. Recently, N self-diffusion was measured in FeN and it was found that the activation energy (E) was considerably lower as compared to other transition metal nitrides [38–40]. Adopting a similar approach [38–40], we prepared a sample [Si (sub.)|$Co^{nat}N$(100 nm)|$Co^{15}N$(2 nm)|$Co^{nat}N$(100 nm)] at T_s = 300 K. Using SIMS, we measured ^{15}N depth profiles from this sample as shown in Fig. 2. They were measured for the as-deposited sample and those annealed isochronally in a vacuum furnace at different temperatures (1 h at each temperature). Due to thermal annealing, ^{15}N profiles get broadened and the width of ^{15}N peak was used to deduce time average diffusivity $D(t) = (\sigma_t^2 - \sigma_0^2)/2t$ [38,39] where σ_t is the standard deviation (before annealing, $t = 0$ and after an annealing time t) obtained after fitting ^{15}N profiles by a single Gaussian function as shown in Fig. 2. Obtained diffusivity (D)

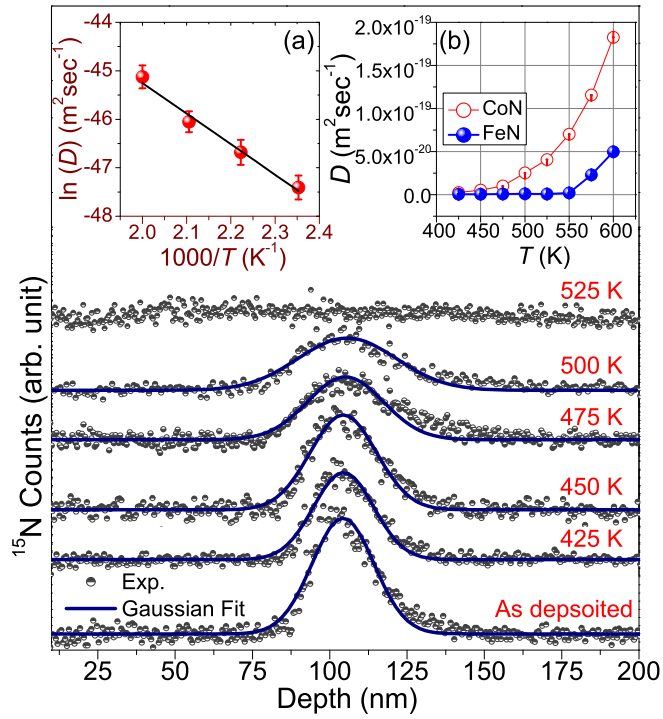

FIG. 2. SIMS depth profile of ^{15}N on a Si (substrate) [$Co^{nat}N$(100 nm)|$Co^{15}N$(2 nm)|$Co^{nat}N$(100 nm)] trilayer after annealing at different temperatures. Inset (a) shows the Arrhenius plot of diffusivity of N. (b) A comparison of N self-diffusion in FeN and CoN. The values of D for FeN is taken from Ref. [38]. The typical error bars in the estimation of diffusivity are the order of the size of the symbols.

TABLE I. Comparison of diffusivity (D, extrapolated to 300 K), activation energies (E), and enthalpy of formation (ΔH_f°) for TiN, CrN (from Refs. [41,51]), FeN (from Ref. [38]) and CoN. The value ΔH_f° for CoN is taken from Ref. [31] while D and E are measured in this work.

Compound	D ($m^2\ s^{-1}$)	E (eV)	ΔH_f° (kJ mol^{-1})
TiN	1.7×10^{-49}	2.2	−338
CrN	1×10^{-55}	2.8	−125
FeN	1.3×10^{-33}	1.5	−47
CoN	4.9×10^{-24}	0.5	0

of N has been measured at different temperatures and follows an Arrhenius type behavior given by:

$$D = D_0 \exp(-E/k_B T). \quad (1)$$

Here, D_0 denotes the pre-exponential factor, E the activation energy, T annealing temperature, and k_B is the Boltzmann's constant.

Using Eq. (1), we get a straight line [as shown in inset (a) of Fig. 2], yielding $E = 0.5 \pm 0.05$ eV. A comparison of N self-diffusion data with other transition metal nitride (TMN) is given in Table I. As compared with other TMN, it can be seen that in CoN, E is smallest signifying that D will be fastest. A comparison of N self-diffusion in FeN [38] and CoN is shown in the inset (b) of Fig. 2. Here, it can be seen that substantial N diffusion already starts above 450 K, whereas in FeN this happens only above 550 K. In stable nitrides like CrN and TiN, appreciable N diffusion takes place at much higher temperatures (>1500 K) [41]. As we can see that ^{15}N profile disappears completely at 525 K (Fig. 2) indicating that N out-diffuses almost completely from CoN. The implication of high T_s on Co-N phases was also amply demonstrated recently [33]. Here, it was shown that when Co was sputtered with different amounts of N_2 (and even with N_2 alone) at 523 K, the resulting phase obtained was always fcc Co, independent of the amount of N_2 that was used during the deposition [33]. This behavior can also be seen from the XRD, SIMS, x-ray photoelectron, and N K-edge x-ray absorption spectroscopy [42] results presented in the Supplemental Material [43] and references [44–50] therein.

From Table I, an analogy can be made between E and enthalpy of formation (ΔH_f°) for several TMN. Thermally stable compounds like TiN and CrN have high E and low ΔH_f°. For the Co_4N phase, $\Delta H_f^\circ \approx 0 \pm 2.9$ kJ mol^{-1} [30,31]. This is quite high as $\Delta H_f^\circ = -338$, -125, and -47 kJ mol^{-1} for TiN, CrN [51], and FeN [52], respectively. Our experimental results on N self-diffusion correlate well with theoretical estimates of ΔH_f° and clearly show that Co-N phases cannot be formed at high T_s. A comparison of ^{15}N depth profiles in FeN and CoN shows that they both look similar and can be fitted to a single Gaussian function even after thermal annealing (Fig. 2). Therefore, N self-diffusion mechanism in CoN should be conventional volume type, similar to FeN [38]. However, in the case of FeN, an anomalous behavior was observed in Fe self-diffusion and explained in terms of fast grain boundary diffusion of Fe [38]. A similar case might also be applicable in CoN, but as no suitable isotope of Co is available, self-diffusion of Co could not be measured.

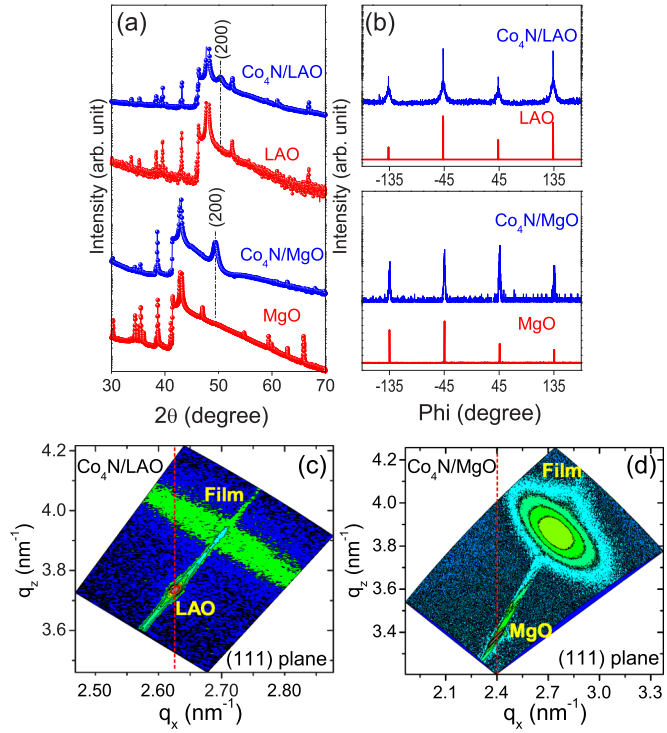

FIG. 3. XRD spectra of Co_4N thin films (a), Phi scan along (111) plane (b) of Co_4N thin film grown on the LAO and MgO substrate. Reciprocal space mapping of Co_4N thin film along the (111) plane grown on the LAO (c) and MgO substrate (d).

The N self-diffusion process obtained for the Co-N system can now be used to understand the formation of Co_4N thin films. We find that in previous works the Co_4N phase was always synthesized at $T_s \geqslant 525$ K [20–27]. Comparing the LP of Co_4N films obtained in those works, we find that the LP was much smaller than the theoretically predicted value of 3.735 Å [18]. For example, Oda *et al.* found LP = 3.59 Å at $T_s = 435$ K [19], Silva and Pandey *et al.* found LP = 3.54 Å, at $T_s = 525$ K [20,33]. In several other studies also, when $T_s >$ 525 K, LP remained at 3.54 Å [21,22]. Therefore, it appears that N diffuses out from Co-N leaving behind fcc Co. The LP of fcc Co is 3.52 Å and the closeness between the LP of Co_4N and fcc Co has lead to the situation in which the fcc Co phase was mistaken for Co_4N. To further prove this analogy, we also deposited samples at different T_s (between 300–400 K) and found that as T_s increases, LP decreases linearly as shown in the Supplemental Material [43].

Under optimized conditions, epitaxial Co_4N thin films were grown on $LaAlO_3$ (LAO) (100) and MgO (100) substrates. They were chosen to understand the role of lattice (mis)matching with Co_4N. The mismatch between Co_4N and LAO is about 1.4% and with MgO it is about 11.3%. XRD patterns show that the films are grown in a single Co_4N phase and highly oriented along the substrate (100) direction, depicted in Fig. 3(a). Out-of-plane LPs comes out to be 3.63 and 3.7 Å, for films grown on LAO and MgO substrates, respectively. To further confirm the epitaxial nature of these films, phi scans along the (111) plane are shown in Fig. 3(b).

Occurrence of fourfold equispaced reflections at 90° in both films confirms the cubic symmetry and epitaxial growth. Moreover, peak positions of films are completely overlapping the substrates peaks, confirming that the unit cell of Co_4N unambiguously grown as cube-on-cube with LAO and MgO unit cells.

Crystalline quality, strain state etc. were investigated using reciprocal space mapping (RSM) measurements illustrated in Figs. 3(c) and 3(d). RSM collected along asymmetric (111) reflection demonstrated that the maps of Co_4N films are far from the pseudomorphic line of the LAO and MgO substrates and corroborate that these films are in a nearly relaxed state with respect to the substrates. Using RSM mapping, we can deduce in-plane LPs. We find that in-plane (out-of-plane) LPs are 3.7(3.63), 3.65(3.7) Å for films deposited on LAO and MgO, respectively. This difference between in-plane and out-of-plane LP can be understood due to tensile strain along the out-of-plane direction for the film grown on LAO and vice versa for the MgO case. Relatively larger lattice mismatch between Co_4N and MgO substrate (−11.3%) is expected to cause an in-plane tensile strain. On the contrary, our film showing a small tensile strain along the out-of-plane direction indicates the existence of strain reversal in Co_4N film grown on the MgO substrate. In addition, the RSMs of these films show some salient features such as elongation of the map in q_X and q_Z directions. Such a larger width of the map can be a characteristic of mosaicity and defined in terms of structural parameters such as lateral correlation length (L), microscopic tilt, and twist disorder etc. [53,54]. Out of these L can be estimated using [53]:

$$L = -\frac{\sin\varphi}{L_3\cos(\xi+\varphi)} \tag{2}$$

where, $\varphi = \tan^{-1}(\frac{q_X}{q_Z})$, $\xi = \tan^{-1}(\frac{\Delta q_X}{\Delta q_Z})$, and $L_3 = \sqrt{\Delta {q_X}^2 + \Delta {q_Z}^2}$.

By utilizing the values of q_X, q_Z and Δq_X, Δq_Z from the RSM maps and using Eq. (2), values of L and microscopic tilt (twist) are calculated. $L \approx 3.3$ for LAO and 1.6 nm for MgO case. Microscopic tilt (twist) disorder was about 0.07(5.3) and 0.1(9.2)° for film grown on LAO and MgO substrates, respectively. As twist is larger than tilt disorder in both films, it signifies the presence of higher density of edge (than screw) type dislocations. In order to measure the dislocation density accurately, one should draw the Williamson's Hall plot for which one needs to use the FWHM of the rocking curves along each reflection. However, in our case, a close estimation of these dislocation densities (ρ_{screw}, ρ_{edge}) can be extracted by utilizing the FWHM of (111) and (200) reflections, respectively, and using the following relations considering the random distribution of dislocations [55]:

$$\rho_{screw(002)} = \frac{\Delta\Omega_{tilt}^2}{4.35|b_{screw}|^2} \tag{3}$$

$$\rho_{edge(111)} = \frac{\Delta\Omega_{twist}^2}{4.35|b_{edge}|^2}, \tag{4}$$

where $\Omega_{tilt/twist}$ are the tile and twist disorder (measured from the FWHM of the rocking curves of symmetric and asymmetric reflections, respectively), $b_{screw/edge}$ are Burgers vectors of the screw and edge dislocations, respectively.

Using above Eqs. (3) and (4), screw (edge) dislocation densities are estimated about 3.4×10^{12} cm^{-2} (6.5×10^{15} cm^{-2}) for LAO and 7×10^{12} cm^{-2} (2×10^{16} cm^{-2}) for MgO grown Co_4N films, respectively. Various reports are available on the heteroepitaxial growth of III-V nitride semiconductor films. Mostly, edge type dislocations density (twist angle) was found to be higher than screw type dislocation (tilt angle). They are typically of the order of 10^9 cm^{-2} for the screw type dislocation and 10^{11} cm^{-2} for the edge type dislocations [56,57]. Compared to these, our obtained values are much higher: 10^{12} cm^{-2} for the screw and 10^{16} cm^{-2} for the edge dislocations. On the other hand, the L in III-V nitrides is generally found to be two orders of magnitude higher compared to the value obtained in the present case. These higher values of dislocation densities and lower values of L obtained in the present study are not surprising as our films were grown at room temperature while the III-V nitride group films usually deposited at higher T_s (>800 K) [56,57]. High substrate temperature will result in better crystallinity, whereas deposition at room temperature leads to a mosaic block epitaxial growth. Presence of mosaicity in both films could be due to the fact that at low T_s (300 K) adatoms would not have sufficient energy to establish the long range ordering to its fullest.

Moreover, difference in the values of L, tilt and twist disorder are subtle in both films (Co_4N on LAO and Co_4N on MgO). Since L is larger and tilt/twist disorder is smaller for the films grown on LAO than that in MgO, it reflects that lattice (mis)match affects the quality of grown films, as expected. In this scenario, we can clearly see that the Co_4N film grown on the MgO substrate has a higher degree of local strain diversity. It is expected that such strain may also affect the magnetic properties and they were investigated using different methods like bulk magnetization, MOKE, and PNR.

From bulk magnetization measurements (shown in Supplemental Material [43]), we found that saturation magnetization (M_s) of both samples is about ≈1200 emu/cm^3 (1 emu/cm^3 = 10^3 A/m). Comparing the experimental values of M_s for Co_4N films obtained so far in the literature, a large variation can be seen ranging between 485–1300 emu/cm^3 [19–21,23–25,28]. As pointed out before, the formation of stoichiometric Co_4N phase itself is questionable, the large difference in M_s can stem from: (i) error in volume measurement of film, (ii) intermixing taking place at the substrate-film interface, (iii) surface oxidation/contamination etc. Among these while (i) may not have a greater influence provided the thickness of film is known accurately, other factors cannot be eliminated when M_s is estimated by bulk magnetization methods. By using magnetic circular dichroism (MCD), M_s can be measured accurately [58]. However, even in a MCD measurement, surface contaminations can affect it. On the other hand, polarized neutron reflectivity (PNR) is a technique which can provide the magnetic depth profile in a nondestructive way and therefore M_s can be measured accurately independent on sample volume etc. In view of this, it is surprising to note that PNR has not been used to measure M_s in Co_4N films.

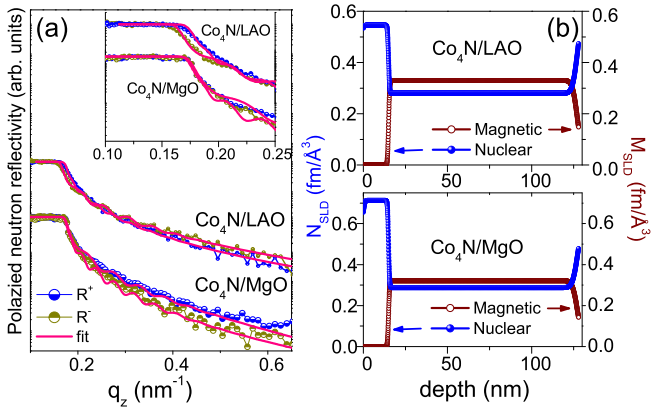

FIG. 4. Fitted PNR spectra of epitaxial Co_4N thin film on LAO and MgO substrates (a). Inset showing the enlarged view of PNR spectra. Respective nuclear SLD (N_{SLD}) and magnetic SLD (M_{SLD}) of epitaxial Co_4N thin films (b).

PNR data of samples grown on LAO and MgO substrates are shown in Fig. 4. Here, the splitting in the reflectivity for spin up (R^+) and down (R^-) neutrons is a measure of magnetization [59]. We can see that at the critical q_z, R^+ and R^- can be distinguished clearly for LAO case but not for MgO. This can be understood by comparing the neutron scattering length density (SLD). The SLD of LAO and MgO is 5.4×10^{-6} and 6.1×10^{-6} Å^{-2}, whereas that of Co_4N (including magnetic SLD) is about 6.2×10^{-6} and -0.4×10^{-6} Å^{-2} for spin up and down neutrons. Since the SLD of substrate exceeds the SLD of Co_4N for the spin down case, R^- will be dominated by the substrate. Nearly comparable values of SLD for MgO and spin up SLD of Co_4N will result in similar R^+ and R^-. Still, the differences in R^+ and R^- at higher q_z would get influenced by M_s and fitting of PNR data (using GenX software [60]) can be used to get both nuclear and magnetic depth profiles as shown in Fig. 4(b). The nuclear density of the Co_4N samples was accurately extracted from the x-ray reflectivity (not shown here) and XRD measurements and used as an input to fit PNR data. From the fitting, we get $M_s = 1.55$ and $1.52(\pm 0.03)$ μ_B/Co atom for films on LAO and MgO, excluding the magnetically dead film-substrate interface (≈5 nm) and surface contaminations (≈3 nm). On the basis of obtained results, we can conclude that the M_s in Co_4N does not get influenced substantially by substrate-film lattice (mis)matching in agreement with previous experimental observations on Fe_4N [61] and Co_4N [20] films grown on different substrates.

Obtained values of M_s are slightly lower than the theoretical value expected for Co_4N. In Co_4N, different Co sites (Fig. 1) show different values of magnetic moments. Corner Co(I) atom exhibits an enhanced moment of 1.967 μ_B and for the face centered Co(II) atoms, it gets reduced to 1.486 μ_B due to hybridization between Co(II) and N. Therefore, the average magnetic moment will be 1.62 μ_B/Co atom in Co_4N (neglecting N moment) [18]. However, in the absence of such enhancement, the magnetic moment of Co(I) would remain at 1.6 μ_B as in bulk Co, and the average magnetic moment would then get reduced to about 1.5 μ_B/Co atom. In the present case,

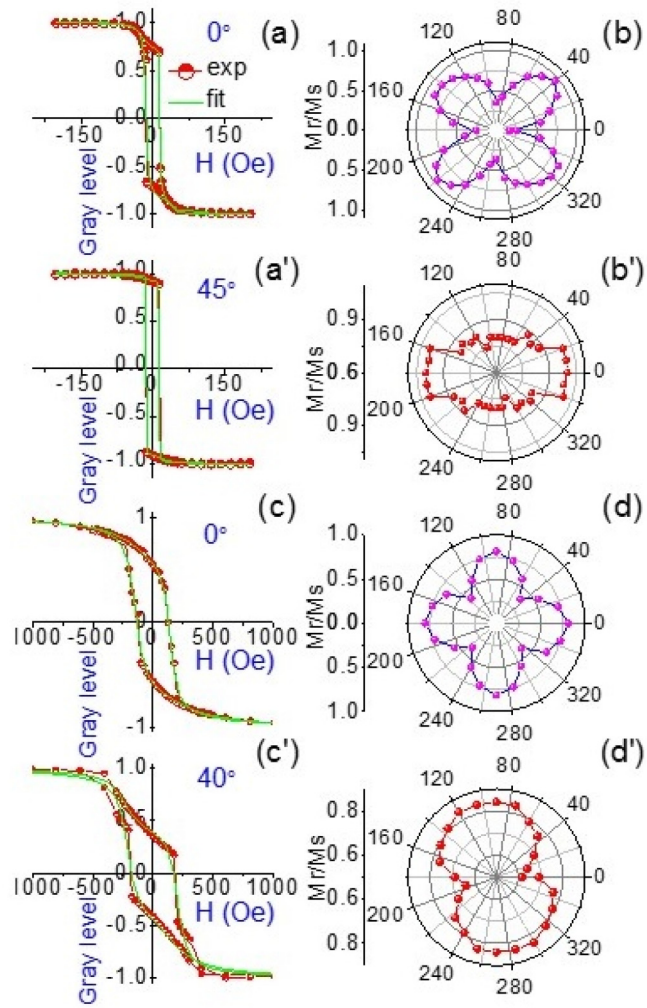

FIG. 5. Longitudinal MOKE hysteresis loops of epitaxial Co_4N thin film on LAO (a and a′). Polar plot of squareness (M_R/M_s) with applied field angle for film grown on LAO (b and b′). Hysteresis loops of epitaxial Co_4N thin film on MgO (c and c′) and MgO substrate (c and c′).

we obtained the average magnetic moment of Co at about 1.55 μ_B/Co atom, which is somewhere between the two cases discussed above. Therefore it can be anticipated that indeed there is some enhancement of the magnetic moment at the Co(I) site. However, as the LP of our samples at 3.70 Å is still lower than the theoretical value of 3.74 Å and significant presence of mosaicity (due to absence of substrate heating) may be the cause of such reduction in M_s.

To study the effect of epitaxy and strain on the magnetic anisotropy, we did MOKE measurements in longitudinal mode. By varying the angle of applied magnetic field direction with reference to sample surface, M-H loops were measured and are shown representatively for 0 and 40° for the film deposited on LAO and MgO in Figs. 5(a) and 5(c). As can be seen, the coercivity (H_c) is much larger in the film deposited on MgO (e.g., at 0°; $H_c \approx 12$ and 130 Oe for films LAO and MgO) and can be understood from the fact that larger local strain diversity would lead to enhanced pinning domains as observed from RSM results discussed above. In addition, the

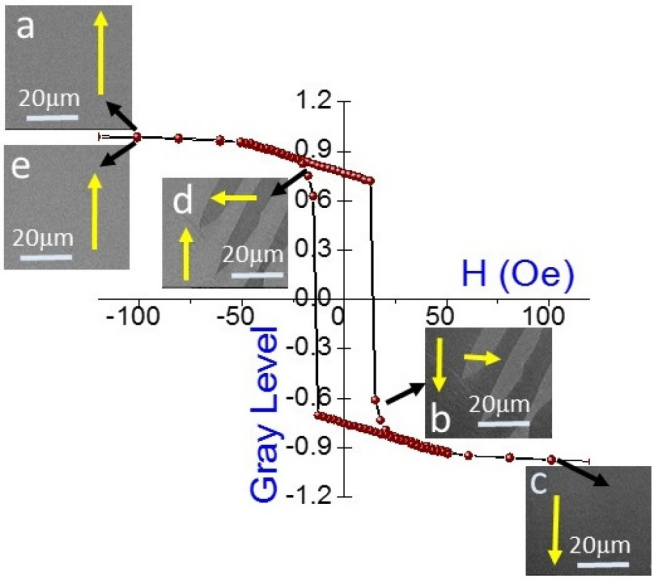

FIG. 6. 20° hysteresis loop of epitaxial Co_4N thin film on LAO substrate and corresponding evolution of Kerr domain images.

shape of M-H loops suggests that two components are present and they can be quantified using [62]:

$$M(H) = \sum_i \frac{2Ms^i}{\pi}\left[\left(\frac{H \pm Hc^i}{Hc^i}\right)\tan\left(\frac{\pi S^i}{2}\right)\right]. \quad (5)$$

From the fitting of M-H loops [using Eq. (5)] for the LAO sample, we obtain these magnetic contributions having $H_c \approx 15$ and 40 Oe and their relative fractions amounting to about 90 and 10%. From the polar plot of squareness ($S = M_R/M_s$; here M_R is the remanence magnetization), it can be seen from Figs. 5(b) and 5(b′) that the major component demonstrates a fourfold, whereas the minor one, a twofold (uniaxial) magnetic anisotropy (MA). The existence of fourfold MA is excepted in the cubic symmetry with easy and hard axes along (100) and (110) directions [16]. On the other hand, the presence of uniaxial MA (UMA) is not expected and can be understood in terms of strain induced anisotropy in agreement with several theoretical [63] and experimental [64] works. Similarly, for the Co_4N film grown on MgO, the superposition of fourfold and UMA can also be seen from Figs. 5(c) and 5(c′). Here, the contribution of UMA is about thrice that in the LAO case. Since we find that the local strain diversity is larger in sample grown on MgO, it may lead to enhanced UMA.

From the M-H loops the magnetocrystalline constant (K_{eff}) can be estimated using: $K_{\text{eff}} = M_s \times H_c/2$ [65]. We find that K_{eff} comes out to be of the order of 10^4 J/m^3 for both samples. This value is quite close to the K_{eff} value observed for epitaxial Fe_4N thin film [16]. Since Fe_4N and Co_4N both possess fourfold anisotropy, K_{eff} is expected to be similar. Furthermore, the magnetization reversal process by 90° domain wall nucleation can be seen when the magnetic field is applied in between easy and hard axes [16]. This can be evidenced in Kerr microscopy images as shown in Fig. 6. Images were captured at points $a(= e)$, b, c, and d and shown there for an applied field angle of 20°. The 180° magnetization reversal can be clearly seen from the image a to e followed by two consecutive 90° domain wall nucleation in image b and d (shown by arrow) for film grown on the LAO substrate. Overall, from the MOKE measurements we can see that strain clearly affects MA in Co_4N films. Greater strain diversity arises due to substrate induced misfit strain observed in films grown on MgO (as compared to LAO) results in loss of fourfold MA giving rise to substantial UMA.

IV. CONCLUSION

In conclusion, we performed N self-diffusion measurements in CoN thin films. We found that N out-diffuses almost completely from CoN at 525 K. Detailed analysis of diffusion data suggests that extrapolated N self-diffusion at 300 K in CoN is more than 10 orders of magnitude faster than that in FeN. Therefore, when the Co_4N phase is grown at $T_s \geqslant$ 525 K, N diffuses-out leaving behind fcc Co. Due to the closeness of LP of Co_4N and fcc Co, it appears that fcc Co was mistaken for Co_4N. By reducing the T_s to 300 K, we have grown stoichiometric Co_4N epitaxial thin films on LAO and MgO substrates. Detailed study of structural and magnetic properties of thus grown Co_4N films suggests that LAO with smaller lattice mismatching (1.4%) has stronger fourfold magnetic anisotropy. Film grown on MgO with about 11% lattice mismatch shows prominent strain diversity resulting in higher UMA and coercivity. The effect of surface contaminations and the interaction between film-substrate interface were quantified by measuring magnetic depth profile using PNR. We found that the magnitude of magnetization does not seem to be greatly affected by lattice mismatching.

ACKNOWLEDGMENTS

N.P. is thankful to Council of Scientific Industrial Research (CSIR) for senior research fellowship (SRF). Authors thank the Department of Science and Technology, India (SR/NM/Z-07/2015) for the financial support and Jawaharlal Nehru Centre for Advanced Scientific Research (JNCASR) for managing the project. A part of this work was performed at AMOR, Swiss Spallation Neutron Source, Paul Scherrer Institute, Villigen, Switzerland. We acknowledge help received from L. Behera in sample preparation and various measurements. M. Horisberger is acknowledged for depositing ^{15}N enriched CoN samples. We are thankful to A. Gome for XRR, R. J. Choudhary and M. Tripathi for S-VSM measurement. We are thankful to A. Wadikar for XPS and R. Sah for XAS measurements.

[1] G. Scheunert, O. Heinonen, R. Hardeman, A. Lapicki, M. Gubbins, and R. Bowman, Appl. Phys. Rev. **3**, 011301 (2016).

[2] B. D. Cullity and C. D. Grahm, *Introduction to Magnetic Materials* (John Wiley & Sons, Inc., Hoboken, 2009).

[3] S. S. Parkin, C. Kaiser, A. Panchula, P. M. Rice, B. Hughes, M. Samant, and S.-H. Yang, Nat. Mater. **3**, 862 (2004).

[4] W. S. Seo, J. H. Lee, X. Sun, Y. Suzuki, D. Mann, Z. Liu, M. Terashima, P. C. Yang, M. V. McConnell, D. G. Nishimura *et al.*, Nat. Mater. **5**, 971 (2006).

[5] J. Coey, H. Sun, and D. Hurley, J. Magn. Magn. Mater. **101**, 310 (1991).

[6] Y. Hou, Z. Xu, S. Peng, C. Rong, J. P. Liu, and S. Sun, Adv. Mater. **19**, 3349 (2007).

[7] C. Yang, L. Jia, S. Wang, C. Gao, D. Shi, Y. Hou, and S. Gao, Sci. Rep. **3**, 3542 (2013).

[8] W.-L. Zuo, X. Zhao, J.-F. Xiong, M. Zhang, T.-Y. Zhao, F.-X. Hu, J.-R. Sun, and B.-G. Shen, Sci. Rep. **5**, 13117 (2015).

[9] J. Coey and P. Smith, J. Magn. Magn. Mater. **200**, 405 (1999).

[10] M. Meinert, J. Phys.: Condens. Matter **28**, 056006 (2016).

[11] S. Kokado, N. Fujima, K. Harigaya, H. Shimizu, and A. Sakuma, Phys. Rev. B **73**, 172410 (2006).

[12] A. Sakuma, J. Magn. Magn. Mater. **102**, 127 (1991).

[13] Y. Imai, Y. Takahashi, and T. Kumagai, J. Magn. Magn. Mater. **322**, 2665 (2010).

[14] B. Yang, L. Tao, L. Jiang, W. Chen, P. Tang, Y. Yan, and X. Han, Phys. Rev. Appl. **9**, 054019 (2018).

[15] Q. Zhang, W. Mi, X. Wang, and X. Wang, Sci. Rep. **5**, 10602 (2015).

[16] J. L. Costa-Krämer, D. M. Borsa, J. M. García-Martín, M. S. Martín-González, D. O. Boerma, and F. Briones, Phys. Rev. B **69**, 144402 (2004).

[17] L. Yin, X. Wang, and W. Mi, ACS Appl. Mater. Interfaces **9**, 15887 (2017).

[18] S. F. Matar, A. Houari, and M. A. Belkhir, Phys. Rev. B **75**, 245109 (2007).

[19] K. Oda, T. Yoshio, and K. Oda, J. Mater. Sci. **22**, 2729 (1987).

[20] C. Silva, A. Vovk, R. da Silva, P. Strichonavec, P. Algarabel, A. Casaca, C. Meneghini, I. Carlomagno, M. Godinho, and M. Cruz, J. Alloys Compd. **633**, 470 (2015).

[21] K. Ito, K. Harada, K. Toko, H. Akinaga, and T. Suemasu, J. Cryst. Growth **336**, 40 (2011).

[22] K. Ito, K. Kabara, T. Sanai, K. Toko, Y. Imai, M. Tsunoda, and T. Suemasu, J. Appl. Phys. **116**, 053912 (2014).

[23] C. Silva, A. Vovk, R. da Silva, P. Strichovanec, P. Algarabel, A. Gonçalves, R. Borges, M. Godinho, and M. Cruz, Thin Solid Films **556**, 125 (2014).

[24] X. Wang, H. Jia, W. Zheng, Y. Chen, and S. Feng, Thin Solid Films **517**, 4419 (2009).

[25] H. Jia, X. Wang, W. Zheng, Y. Chen, and S. Feng, Mater. Sci. Eng.: B **150**, 121 (2008).

[26] H. Asahara, T. Migita, T. Tanaka, and K. Kawabata, Vacuum **62**, 293 (2001).

[27] J.-S. Fang, L.-C. Yang, C.-S. Hsu, G.-S. Chen, Y.-W. Lin, and G.-S. Chen, J. Vac. Sci. Technol. A **22**, 698 (2004).

[28] H. Li, Y. Zhang, K. Yang, H. Liu, X. Zhu, and H. Zhou, Appl. Surf. Sci. **406**, 110 (2017).

[29] M. Lourenço, M. Carvalho, P. Fonseca, T. Gasche, G. Evans, M. Godinho, and M. Cruz, J. Alloys Compd. **612**, 176 (2014).

[30] Y. Imai, M. Sohma, and T. Suemasu, J. Alloys Compd. **611**, 440 (2014).

[31] X. Zhao, L. Ke, C.-Z. Wang, and K.-M. Ho, Phys. Chem. Chem. Phys. **18**, 31680 (2016).

[32] A. Tayal, M. Gupta, N. P. Lalla, A. Gupta, M. Horisberger, J. Stahn, K. Schlage, and H.-C. Wille, Phys. Rev. B **90**, 144412 (2014).

[33] N. Pandey, M. Gupta, R. Gupta, S. Chakravarty, N. Shukla, and A. Devishvili, J. Alloys Compd. **694**, 1209 (2017).

[34] N. Pandey, M. Gupta, R. Gupta, P. Rajput, and J. Stahn, J. Magn. Magn. Mater. **448**, 274 (2018).

[35] R. Gupta, N. Pandey, A. Tayal, and M. Gupta, AIP Adv. **5**, 097131 (2015).

[36] J. Stahn and A. Glavic, Nucl. Instrum. Methods Phys. Res. A **821**, 44 (2016).

[37] J. Stahn and A. Glavic, J. Phys.: Conf. Ser. **862**, 012007 (2017).

[38] A. Tayal, M. Gupta, A. Gupta, P. Rajput, and J. Stahn, Phys. Rev. B **92**, 054109 (2015).

[39] M. Gupta, A. Tayal, A. Gupta, R. Gupta, J. Stahn, M. Horisberger, and A. Wildes, J. Appl. Phys. **110**, 123518 (2011).

[40] M. Gupta, A. Gupta, S. Rajagopalan, and A. K. Tyagi, Phys. Rev. B **65**, 214204 (2002).

[41] L. Hultman, Vacuum **57**, 1 (2000).

[42] D. M. Phase, M. Gupta, S. Potdar, L. Behera, R. Sah, and A. Gupta, AIP Conf. Proc. **1591**, 685 (2014).

[43] See Supplemental Material at http://link.aps.org/supplemental/10.1103/PhysRevB.99.214109 for describing the growth of stochiometric Co_4N thin films and their basic characterizations. The structural and electronic properties are studied.

[44] H. Zhang, J. Poole, R. Eller, and M. Keefe, J. Vac. Sci. Technol. A **17**, 1904 (1999).

[45] C. Cabral Jr., K. Barmak, J. Gupta, L. Clevenger, B. Arcot, D. Smith, and J. Harper, J. Vac. Sci. Technol. A **11**, 1435 (1993).

[46] S. Ram, Mater. Sci. Eng.: A **304–306**, 923 (2001).

[47] W. Diekmann, G. Panzner, and H. Grabke, Surf. Sci. **218**, 507 (1989).

[48] B. Ravel and M. Newville, J. Synchrotron Radiat. **12**, 537 (2005).

[49] T. I. Morrison, M. B. Brodsky, N. J. Zaluzec, and L. R. Sill, Phys. Rev. B **32**, 3107 (1985).

[50] S. Berg, E. Särhammar, and T. Nyberg, Thin Solid Films **565**, 186 (2014).

[51] W. F. Gale and T. C. Totemeier, *Smithells Metals Reference Book* (Elsevier Butterworth-Heinemann, Oxford, 2003).

[52] F. Tessier, A. Navrotsky, R. Niewa, A. Leineweber, H. Jacobs, S. Kikkawa, M. Takahashi, F. Kanamaru, and F. J. DiSalvo, Solid State Sci. **2**, 457 (2000).

[53] S. Pereira, M. Correia, E. Pereira, K. O'Donnell, E. Alves, A. Sequeira, N. Franco, I. Watson, and C. Deatcher, Appl. Phys. Lett. **80**, 3913 (2002).

[54] W.-X. Ni, K. Lyutovich, J. Alami, C. Tengstedt, M. Bauer, and E. Kasper, J. Cryst. Growth **227-228**, 756 (2001), Proceeding of the Eleventh International Conference on Molecular Beam Epitaxy.

[55] C. Dunn and E. Kogh, Acta Metall. **5**, 548 (1957).

[56] R. F. Davis, T. Gehrke, K. Linthicum, P. Rajagopal, A. Roskowski, T. Zheleva, E. A. Preble, C. Zorman, M. Mehregany, U. Schwarz *et al.*, Materials Research Society Internet Journal of Nitride Semiconductor Research **6**, e14 (2001).

[57] M. Kneissl, T. Kolbe, C. Chua, V. Kueller, N. Lobo, J. Stellmach, A. Knauer, H. Rodriguez, S. Einfeldt, Z. Yang *et al.*, Semicond. Sci. Technol. **26**, 014036 (2010).

[58] K. Ito, K. Harada, K. Toko, M. Ye, A. Kimura, Y. Takeda, Y. Saitoh, H. Akinaga, and T. Suemasu, Appl. Phys. Lett. **99**, 252501 (2011).

[59] S. Hope, J. Lee, P. Rosenbusch, G. Lauhoff, J. A. C. Bland, A. Ercole, D. Bucknall, J. Penfold, H. J. Lauter, V. Lauter, and R. Cubitt, Phys. Rev. B **55**, 11422 (1997).

[60] M. Björck and G. Andersson, J. Appl. Crystallogr. **40**, 1174 (2007).

[61] K. Ito, G. H. Lee, K. Harada, M. Suzuno, T. Suemasu, Y. Takeda, Y. Saitoh, M. Ye, A. Kimura, and H. Akinaga, Appl. Phys. Lett. **98**, 102507 (2011).

[62] M. B. Stearns and Y. Cheng, J. Appl. Phys. **75**, 6894 (1994).

[63] T. Burkert, O. Eriksson, P. James, S. I. Simak, B. Johansson, and L. Nordström, Phys. Rev. B **69**, 104426 (2004).

[64] M. C. dos Santos, J. Geshev, L. G. Pereira, M. C. M. Alves, J. E. Schmidt, and P. Allongue, Phys. Rev. B **70**, 104420 (2004).

[65] N. Ji, M. S. Osofsky, V. Lauter, L. F. Allard, X. Li, K. L. Jensen, H. Ambaye, E. Lara-Curzio, and J.-P. Wang, Phys. Rev. B **84**, 245310 (2011).